Journal of Fluorescence (2023) 33:1227–1236
https://doi.org/10.1007/s10895-023-03180-9

RESEARCH

The Novel 5-Fluorouracil Loaded Ruthenium-based Nanocarriers Enhanced Anticancer and Apoptotic Efficiency while Reducing Multidrug Resistance in Colorectal Cancer Cells

Ferdane Danişman-Kalindemirtaş[1] · Dilşad Özerkan[2] · İshak Afşin Kariper[3] · Huri Bulut[4]

Received: 11 January 2023 / Accepted: 11 February 2023 / Published online: 22 February 2023
© The Author(s), under exclusive licence to Springer Science+Business Media, LLC, part of Springer Nature 2023

Abstract

Recently, nanocarriers have been made to eliminate the disadvantages of chemotherapeutic agents by nanocarriers. Nanocarriers show their efficacy through their targeted and controlled release. In this study, 5-fluorouracil (5FU) was loaded into ruthenium (Ru)-based nanocarrier (5FU-RuNPs) for the first time to eliminate the disadvantages of 5FU, and its cytotoxic and apoptotic effects on HCT116 colorectal cancer cells were compared with free 5FU. 5FU-RuNPs with a size of approximately 100 nm showed a 2.61-fold higher cytotoxic effect compared to free 5FU. Apoptotic cells were detected by Hoechst/propidium iodide double staining, and the expression levels of BAX/Bcl-2 and p53 proteins, in which apoptosis occurred intrinsically, were revealed. In addition, 5FU-RuNPs was also found to reduce multidrug resistance (MDR) according to BCRP/ABCG2 gene expression levels. When all the results were evaluated, the fact that Ru-based nanocarriers alone did not cause cytotoxicity proved that they were ideal nanocarriers. Moreover, 5FU-RuNPs did not show any significant effect on the cell viability of normal human epithelial cell lines BEAS-2B. Consequently, the 5FU-RuNPs synthesized for the first time may be ideal candidates for cancer treatment because they can minimize the potential drawbacks of free 5FU.

Keywords Ruthenium-based nanoparticles · 5FU · Colorectal cancer · Apoptosis · Cytotoxicity

Introduction

Colorectal cancer is one of the most common and malignant cancers, and chemotherapy and colectomy are mainly used for treatment. In recent years, the number of colorectal cancers has increased worldwide [1]. Despite the remarkable progress in the treatment of colorectal cancer, the poor properties of drugs such as solubility, dispersion, permeability, and bioavailability, as well as the development of drug resistance, have a negative impact on treatment [2, 3]. For all these reasons, the search for new treatment options continues. Nowadays, nanodevices consisting of nanoscale materials such as proteins, protein complexes, tissues, chromosomes, lipids, carbohydrates, and metals are used for the diagnosis and treatment of diseases. Due to the complexity of cancer, numerous treatments are still being attempted, but none of them can guarantee survival. However, nanoparticles have many advantages, such as drug delivery vehicles, controlled release at the target site, and high drug concentrations that prevent potential side effects [4]. Due to the enhanced permeability and retention (EPR) effect, nanoparticles in the 10–200 nm range tend to accumulate in tumor tissue by passive targeting. This is because the endothelium of tumor tissue has increased permeability compared to the endothelium of normal tissue. Therefore, passive tumor targeting takes place as this accumulation cannot occur in normal tissue [5]. In addition, the lack of a lymphatic drainage system in tumor tissue ensures that nanoparticles do not become trapped in the reticuloendothelial system [4]. The fact that nanoparticles are smaller than 200 nm offers many advantages over conventional chemotherapy, such as

✉ Dilşad Özerkan
dilsadokan@gmail.com

1 Faculty of Medicine, Department of Physiology, Erzincan Binali Yıldırım University, Erzincan, Turkey

2 Faculty of Engineering and Architecture, Department of Genetic and Bioengineering, Kastamonu University, Kastamonu, Turkey

3 Department of Science Education, Erciyes University, Education Faculty, Kayseri, Turkey

4 Faculty of Medicine, Department of Biochemistry, İstinye University, Istanbul, Turkey

increased drug uptake, longer circulation time, reduced drug resistance, targeted therapy, and controlled release [6]. Drug delivery systems can extend the physiological circulation time of drugs and increase targeted drug delivery. Delayed and controlled release systems can reduce side effects by regulating drug bioavailability and maintaining drug concentration at specific time intervals [7]. Drug release is crucial for improving the therapeutic efficacy of drug-loaded nanoparticles and reducing dose-dependent toxicity [8, 9]. Various NPs can enhance the efficacy of 5FU in colon cancer cell lines [10].

Complexes of metals and heterocyclic ligands are of particular interest in bioinorganic chemistry because they are model compounds of metal proteins. In recent years, inorganic drugs have formed an important part of medical therapeutics, and the synthesis of N-coordinated metal complexes has been intensively studied in coordination chemistry [11–13]. Ruthenium is preferred because it has low toxicity to normal cells, is more readily absorbed by tumor cells, and is easily excreted from the body [13]. One of its main advantages is that it selectively targets and binds the patient's tissues, especially thanks to its ligand structure [14]. Unlike platinum, it has shown therapeutic effect in tumors resistant to cisplatin by binding to DNA crosslinks at different sites [15]. Despite all these properties, studies on Ru-based nanoparticles are still nascent and very limited [16–19]. For cancer prevention, the synthesis and development of new molecules is very important for the selection and direct elimination of the target. As far as we know, RuNPs have been synthesized and studied for their various properties, but drug-loaded Ru nanocarriers have not been found in the literature. Moreover, only the cytotoxic effects of RuNPs have been evaluated by [20]. 5FU is an important anticancer agent that is frequently used in many types of cancer. Although the mechanism of action is still being investigated, various studies are carried out to investigate its effectiveness against cancer. However, drug resistance limits the clinical use of 5FU [21]. For these reasons, we searched for new drug delivery systems that would increase the effectiveness of 5FU. In this study, ruthenium nanocarrier loaded with 5FU was synthesized for the first time and the effects of this nanocarrier on cancer cells were investigated. Additionally, the activity of free 5FU and 5FU-RuNPs on HCT116 colon cancer cell viability was compared.

Materials

$RuCl_3$ (Ruthenium (III) chloride), $NaBH_4$ (Sodium borohydride) and SDS (Sodium dodecyl sulfate) (Sigma Aldrich) used in the study were taken in analytical purity. Dialysis tubing cellulose membrane (Sigma Aldrich Company) was performed in drug release analyzes. Dulbecco's Modified Eagle Medium (DMEM) (Gibco, Thermofisher Scientific), Fetal bovine serum (FBS) (Sigma Aldrich), penicilin-streptomicin (pen/strep) (Gibco, Thermofisher Scientific), and Sulforhodamine (SRB) (Sigma Aldrich) solution were used for cell culture analyzes. Hoescht33342 (ThermoFisher) and Propidium Iodide (PI) (BioLegend) were utilized in immunofluorescence analyzes. Anti-Beta actin (Cell signaling, 4970, USA), anti-BCRP/ABCG2 (Abcam, 130244, UK), anti-p53 (Abcam, 32389, UK), anti-Bax (Elabscience, E-AB-13814, USA), anti-Bcl2 (GeneTex, GTX100064, USA) primary antibodies and the secondary antibody (Santa Cruz Biotechnology, Inc., Santa Cruz Ca USA) were used in Western Blotting.

Methods

Preparation of Nano-drug Composite

A wet chemical method (chemical reduction method) was used for the synthesis of Ru nanoparticles. A stock solution was prepared by dissolving 0.1 mM $RuCl_3$ in 50 mL of water. After the stock solutions of 3 mM $NaBH_4$ and 2 mM SDS were prepared, equal volumes (1:1:1 w/w-Ru:$NaBH_4$:SDS) of all stock solutions were placed in a beaker and mixed with a magnetic stirrer for 15 min. The solution was used as a RuNP stock solution [22]. 5-FU was dissolved in water at a concentration of 1 mg/mL as 5-FU stock solution. The resulting NanoRu stock solution was mixed with the 5-FU solution previously prepared in aqueous medium at a concentration of 1 mg/mL (1:1 w/w- RuNano:5-FU). The mixture was sonicated in an ultrasonic bath at room temperature for 15 min. The structure of the 5FU-RuNP structure is shown in Fig. 1.

Characterization of Ruthenium-based Nanoparticles

Zeta Sizer Measurements

Zeta sizer measurements were made at room temperature. Dimensional analysis of Ru samples was performed by dynamic light scattering (DLS) measurements using Zetasizer Nano ZS using 4 mW He–Ne laser operating at a wavelength of 633 nm and a detection angle of 173°.

Energy Dispersive X-ray Analysis (EDX)-Field-Emission Scanning Electron Microscopy (FE-SEM) Analyses

For FE-SEM and EDX analysis, RuNPs and 5FU-RuNPs samples were dropped on glass substrate and coated with Au/Pd at 45 A^0 thickness by Polaron sc 7620 mini sputter coater device. Regarding liquid samples' analysis, imaging

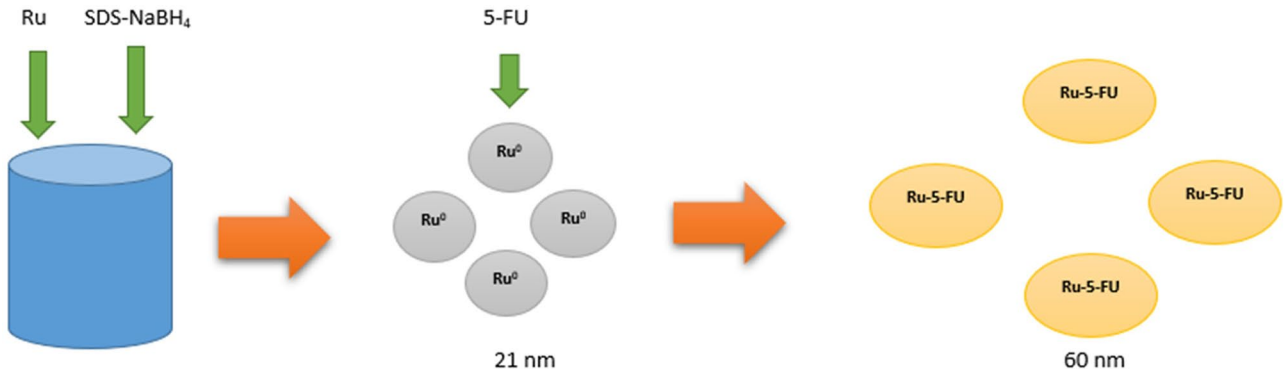

Fig. 1 Schematic construction of 5FU-RuNPs

was performed by dropping on glass substrates and putting on the device after drying.

Absorption Measurements

Absorption of aqueous solutions of synthesized materials was measured with Hach Lange DR 5000 Spectrophotometer. Measurements were taken in the wavelength range of 200–1100 nm using water as a reference for the reference part of the spectrophotometer and the solutions prepared for the sample part.

Drug Release Analysis

5FU medication release from NPs was studied in vitro in buffer solutions (pH 7.4) at 37 ± 0.5 °C using a dialysis tubing cellulose membrane (average flat width 10 mm) (0.4 in.) and PBS buffer solution. 5FU drug loaded on 1 mg/mL nanocarrier was transferred to 2 ml dialysis membrane. Dialysis membrane size is approximately 16 cm, ambient temperature is approximately 37 ± 0.5 °C. Both ends of the dialysis membrane were closed. 5FU loaded on the nanocarrier in the dialysis membrane was left in 50 ml of buffer solution with pH: 7.4, and the release was followed for 50 h. 5 different concentrations were prepared with 5FU drug and their absorbance at 290 nm was determined by UV spectrophotometer.

Cell Culture Tests

The human colon cell line (ATCC) HCT116 was selected for this study. Cells were grown in DMEM with 10% FBS and 1% Pen/Strep in T75 culture flasks, and the degree of confluence of the cells was set at 80%. Then, 5000 cells were seeded in 96 wells and incubated at 5% CO_2 and 37 °C. For the next day treatment, 6 different doses (0.7, 1.4, 2.8, 5.6, 11.25, and 22.5 µl) of free 5FU, RuNPs, and 5FU-RuNPs were added to them and incubated again for 48 h. After 48 h, the antiproliferative activity of free 5FU, RuNPs and 5FU-RuNPs against colon cancer cell line (HCT116) was analyzed at least three times by SRB assay. The sulforhodamine B (SRB) assay does not show metabolic activity like 3-(4,5-dimethylthiazol-2-yl)-2,5-diphenyltetrazolium bromide (MTT). Instead of metabolic activity, SRB binds mainly stoichiometrically to proteins with this dye, so living cells can be determined [23]. Human epithelial cells (BEAS-2B) were used as healthy controls, and cell viability was measured on this group.

Dose–response curves were generated to calculate the IC_{50} (concentration that inhibits the growth of 50% of cells) of the RuNPs. This parameter was used to compare the efficacy of the 5FU-RuNPs.IC_{50} Calculator (AAT Bioquest) was used for IC_{50} calculation (https://www.aatbio.com/tools/ic50-calculator).

HOESCHT/PI Double Staining

HCT116 cells were seeded on 96-well plates with 5000 cells/100 µl in each well. IC_{90} levels of free 5FU, RuNPs, and 5FU-RuNPs were administered, and after 24 h, the Hoescht33342/ PI staining protocol was used. 50 µL of the two dyes were added to the wells, from which supernatants were taken from the working solution prepared at 1 µg/mL and incubated at room temperature in the dark. Photographs were taken using a Nikon Eclipse Ts2 immunofluorescence microscope.

Western Blot Analysis

In the cell lysates, the amount of total protein was determined by the Bradford method in a plate reader (Thermo Scientific Multiskan FC, 2011–06, USA) at a wavelength of 595 nm. 1 mg/ml bovine serum albumin (BSA) was used as a standard. For each sample, approximately 20 µg of total protein was loaded into SDS-PAGE and run at 120 mV for 1 h. Transfer of protein samples in the gel onto

PVDF membranes was performed using the transfer device (Biorad, USA) (incubation at 110 mV for 10 min). For the blocking process of the membranes, they were incubated in 5% skim milk at room temperature in an orbital shaker for 1 h. After blocking, the membranes were washed 5 times for 5 min with TBS -T.

The primary antibodies anti-beta-actin, anti-BCRP/ABCG2, anti-P53, anti-Bax, and anti-Bcl2 were prepared in 2.5% skim milk at ratios of 1/1000, 1/500, 1/750, 1/200, and 1/200, respectively. After labeling the membranes with the primary antibodies, they were incubated overnight at + 4 °C. After washing the membranes with TBS -T, they were labeled with the secondary antibodies prepared at a ratio of 1/1000 and incubated at room temperature for one hour. The antibody bands were visualized and analyzed on the Vilbert Laurmart Fusion Fx5 instrument.

Statistical Analysis

Experiments were repeated at least three times, and results were presented as mean ± standard deviation (SD). Between the groups, Kruskal–Wallis and one-way analysis of variance (ANOVA) tests were performed using GraphPad Prism version 5 software. $p < 0.05$ considered to be significant and $p < 0.01$ considered to be significant remarkably.

Results and Discussion

The Results of the Characterization of 5FU-RuNPs were Determined Suitable to Penetrate into HCT116 Cells

While the specific peak of Ru nanoparticles [24] was detected at 280 nm according to UV–VIS Spectrum, this peak shifted to 291 nm when 5FU was bound to RuNPs (Fig. 2). This absorption peak, resulting from charge transfer from the oxygen atom to ruthenium at 280 nm, shifted to the visible region at 291 nm due to the interaction of ruthenium with electro-negative atoms such as F, N, or O in 5FU. While the electronic π-π* transitions of the 5FU molecule are observed at 230 nm in the literature due to the aromatic ring and double bonds, they were detected at 233 nm in this study due to the solvent effect and RuNPs (i.e., environmental effects) [25]. Since it was not measured in a vacuum environment of 200 nm and below, it was not evaluated.

As mentioned earlier, the measurements were performed using the Zetasizer Nano ZS instrument. Each sample was measured three times, and the average of the three measurements was obtained. Figure 3 shows that the size distribution of RuNPs ranged from 13.54 nm to 68.06 nm. However, nanoparticles larger than 100 nm were not detected. While the mean particle size was measured at 21 nm, the derived count rate was 90 (PDI: 0.607). The size distribution ranged from 37.84 nm to 122.4 nm when

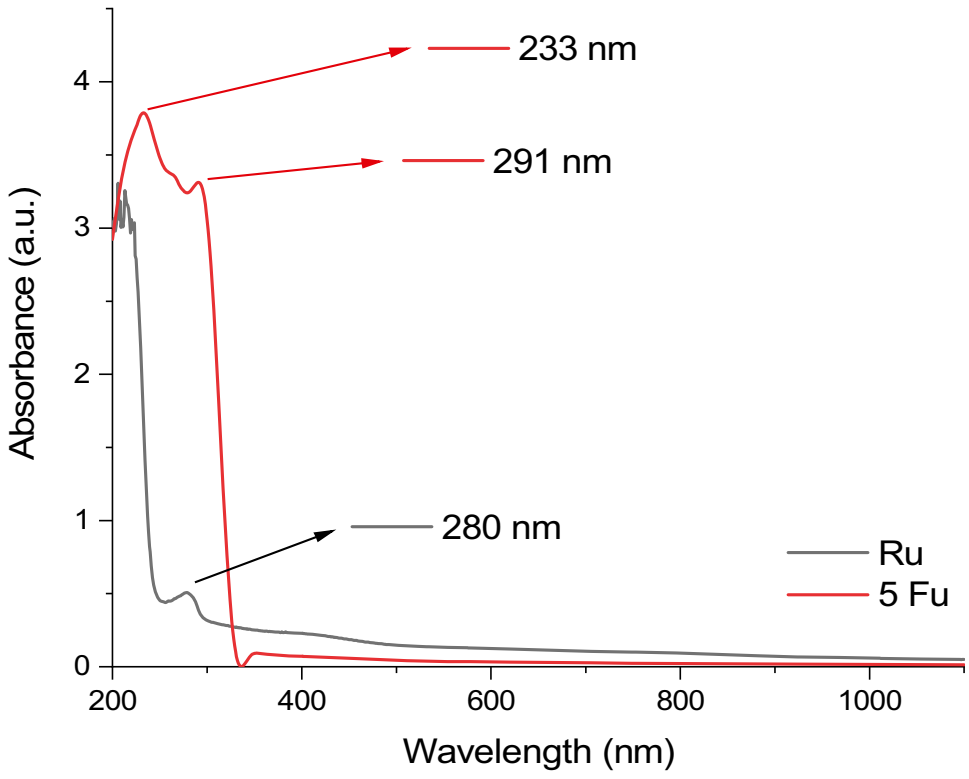

Fig. 2 UV–VIS spectrum of RuNPs and 5FU-RuNPs

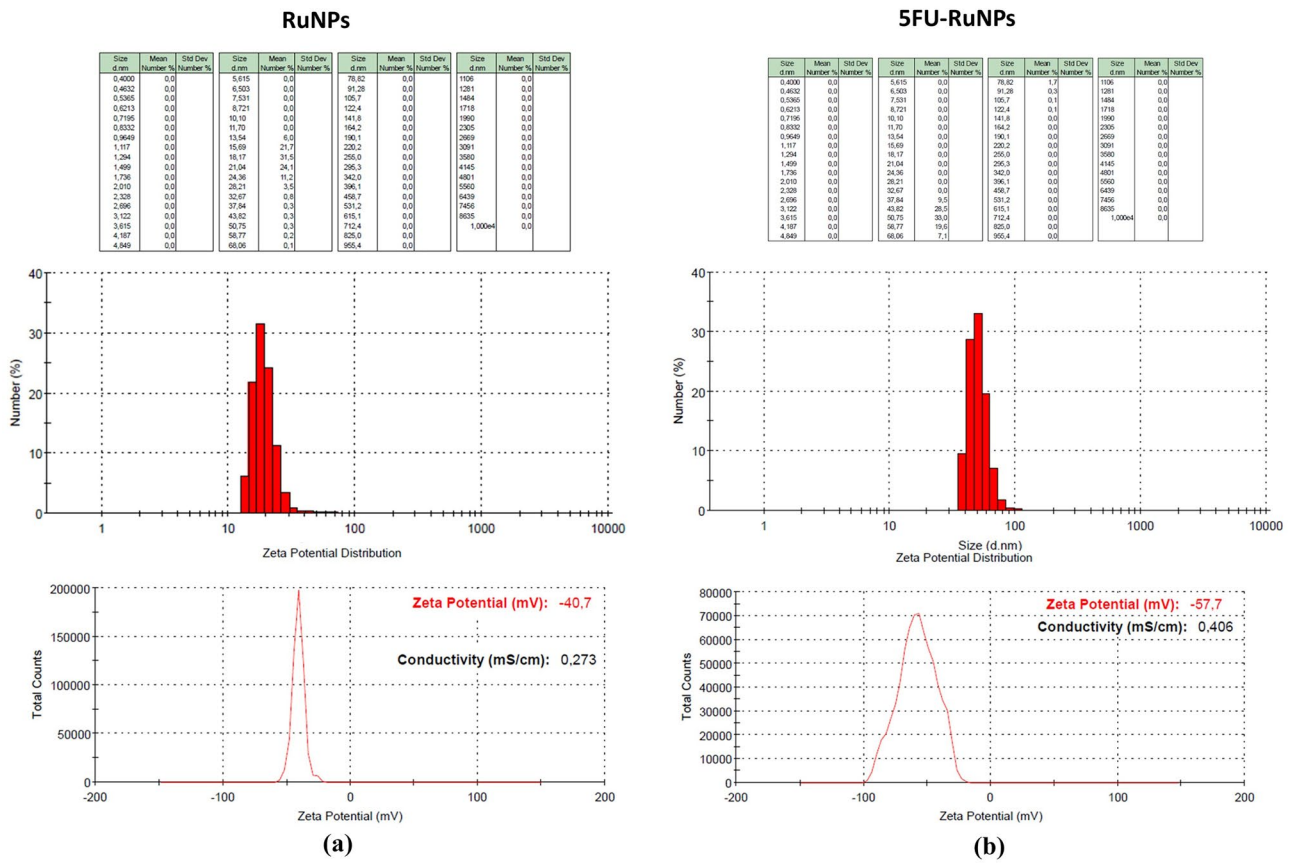

Fig. 3 ZetaSizer spectrums of **a** RuNPs and **b** 5FU-RuNPs

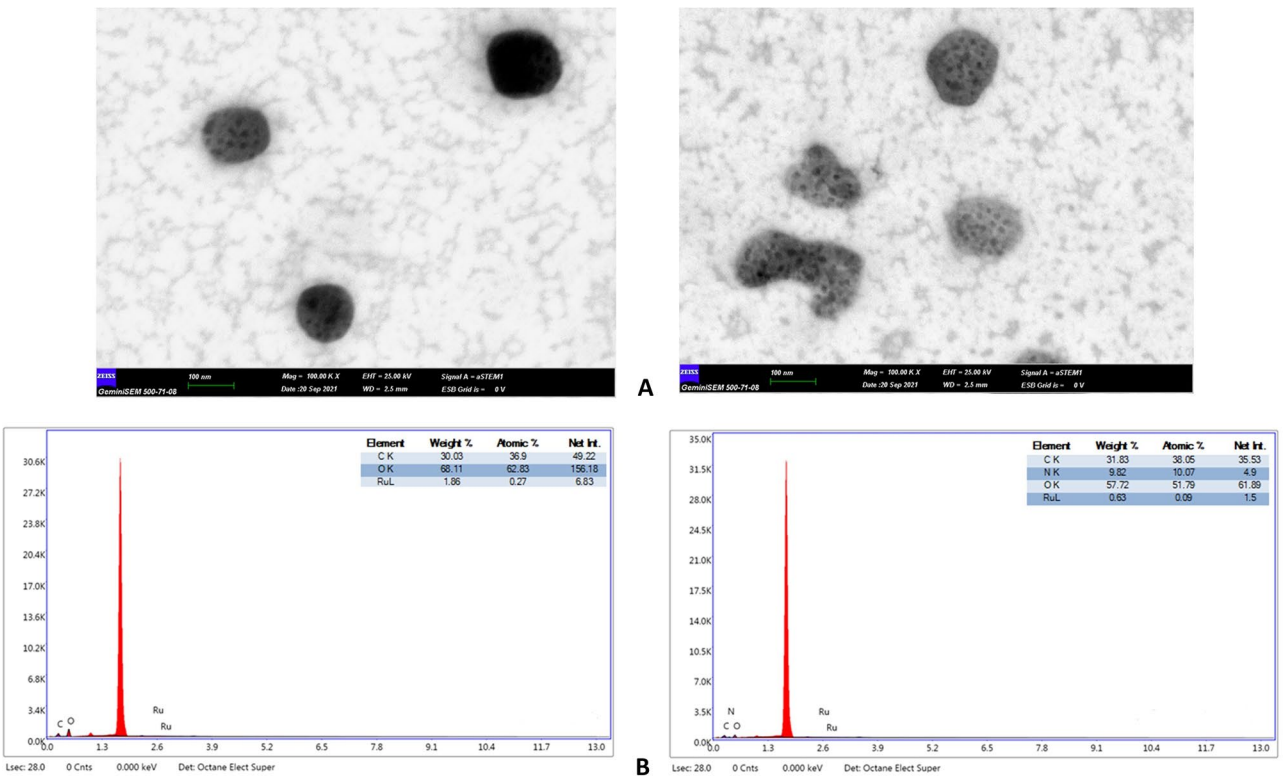

Fig. 4 **a** FE-SEM images **b** EDX spectrums of RuNPs and 5FU-RuNPs

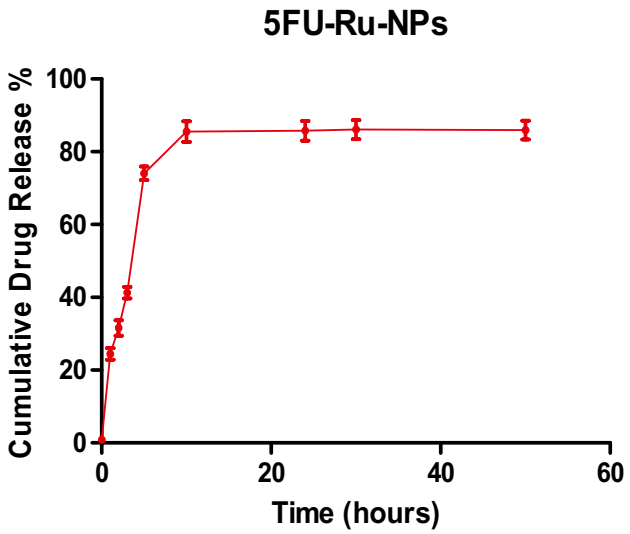

Fig. 5 Cumulative drug release of 5FU from 5FU-RuNPs

5FU was bound to RuNPs. The average particle size was 50–60 nm. The derived count rate was 60 (PDI: 0.589). An increase in particle size was observed when 5 FU was bound to RuNPs. While the surface potential of RuNPs was -40.7 mV, it increased to -57.7 mV when 5FU was bound. However, the conductivity of the solution also increased. The change in surface potential also affected the Krebs assays. Looking at the count rate values, it can be seen that although the number of nanoparticles in the environment decreased, more mature nanoparticles were formed compared to the PDI values.

When examining FE-SEM and EDX data, it was found that, except for the strong peak of Si substrate material, C and O RuNPs originated from SDS, while the relative proportions of these elements increased when 5FU was bound (Fig. 4a). A decrease was observed in the amount of Ru. According to the images from FE-SEM, RuNPs were observed at 100 nm and below, while nanoparticles were detected at 100 nm and at the edges when 5FU was bound (Fig. 4b). It is normal to observe such agglomerations when nano solutions, usually prepared as aqueous solutions in FE-SEM analyzes, are dried on the glass substrate in a sterile environment at room temperature overnight. However, the results are consistent with the zeta sizer aspect ratios.

Drug Release Studies of 5FU-RuNPs were Found Effective

To evaluate the drug release profile, drug release from the nanocarrier loaded with 5FU was performed at physiological pH, pH 7.4. According to the UV results, the wavelength of the 5FU anticancer drug was determined as 290 nm. From the measurements performed at different time points at this wavelength, the release of 5FU from the Ru nanocarrier is cumulative, especially in the first 10–12 h, and the release percentage reaches about 85% within 12 h (Fig. 5). According to the UV results, there appears to be a gradual increase in the cumulative 5FU release rate from 5FU-RuNPs over time. In addition, the fact that 5FU from RuNPs has a high release rate of 85% is important for the drug effect to reach the targeted cancer cells at a high rate.

5FU-RuNPs Significantly Decreased Cell Viability

5FU is a cancer drug with proven efficacy and is especially preferred in the treatment of colorectal cancer. However, it has many disadvantages, such as short half-life [26], rapid diffusion into tumor tissue, retention of 5FU in CRC [27], rapid degradation in the body, the need for higher doses for

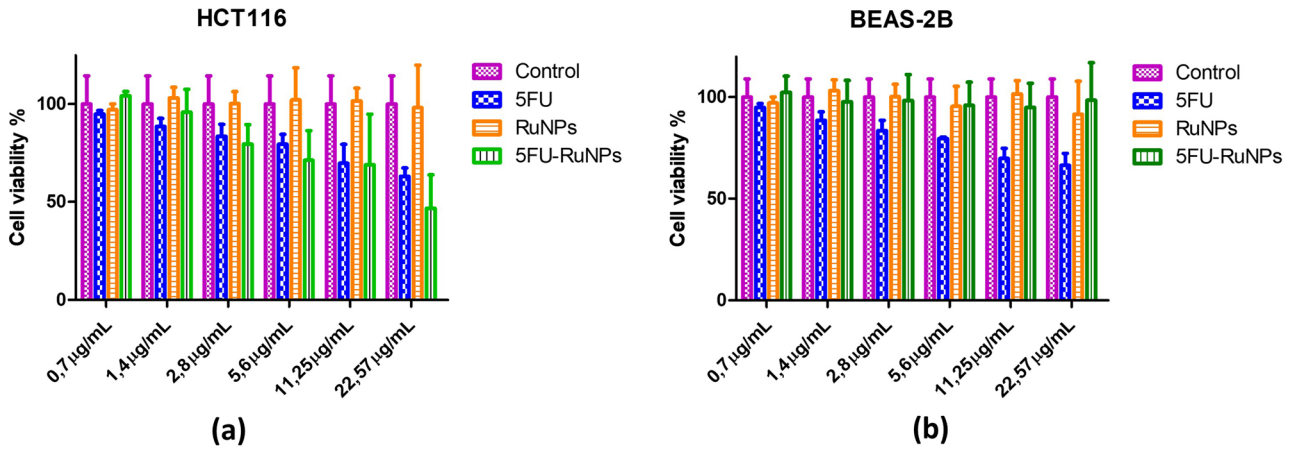

Fig. 6 The graphic shows the difference between all group's viabilities in each dose after 48 h. **a** HCT116. $p = 0.0054$. **b** BEAS-2B. $p = 0.0033$. $n = 3$, $p < 0.01$ compared with control

Table 1 Comparison of IC_{50} values of free 5FU and 5FU-RuNPs treated HCT116 groups

Groups	IC_{50} values (µg/mL)
Free 5FU	51.8897
5FU-RuNPs	**19.8122**

more effective results [28], and high treatment costs [29]. The main goal is to minimize or eliminate these drawbacks to increase treatment success. Therefore, nanocarriers are ideal candidates for this purpose.

22.5 µg/mL 5FU most effectively inhibited cell growth of HCT116 cells (Fig. 6a). It is evident that 5FU-RuNPs are more effective than free 5FU. In this study, the cytotoxic effect of RuNPs not loaded with 5FU on HCT116 colon carcinoma cells and normal BEAS-2 control cells was also investigated, and no significant cytotoxic effect was found. These results indicate that metal based RuNPs are not toxic. Studies have shown that ruthenium complexes have very low toxicity in healthy tissues [30, 31]. BEAS-2B cells, the healthy control group, were also not significantly affected by free 5FU, RuNPs, and 5FU-RuNPs (Fig. 6b). All groups were compared with the control group and statistical significance was found between the groups with free 5FU and 5FU-RuNPs ($p = 0.0183$, $p < 0.05$). According to the IC_{50} values of HCT116 cells, the IC_{50} of free 5FU was 51.8897 µg/ml, while the IC50 of 5FU-RuNPs was 19.8122 µg/ml (Table 1). According to our findings, it is noteworthy that 5FU-RuNPs are 2.6 times more effective than free 5FU. Accordingly, the side effects of 5FU are reduced by treatment with a lower dose of the drug. Considering the results, the novel Ru nanocarrier enhances the effect of 5FU and provides a promising option for cancer treatment.

On the other hand, the 5FU-RuNPs did not show significant cytotoxicity on BEAS-2B cells. For this reason, IC_{50} and IC_{90} calculations could not be performed, and Western blotting and Hoescht/ PI staining were not performed with BEAS-2 cells.

Apoptosis was Increased with 5FU-RuNPs Effect in Colorectal Cells

Hoechst 33342, a stain for the nuclei of living cells, and PI, a fluorescent stain for DNA in cells, are used to determine cell survival. PI binds mainly double-stranded nucleic acids in apoptosis, necrosis, and fixed cells, but cannot cross the membrane of living cells [32]. After the application of 5FU-RuNPs, apoptosis was significantly increased in contrast to the control group. When the group treated with 5FU was compared with the group treated with 5FU-RuNPs, a lower percentage of dead cells was observed (Fig. 7). Moreover, apoptosis in HCT116 cells was increased by using a lower concentration of 5FU in a Ru nanocarrier loaded with 5FU.

Apoptosis-related Proteins were Found Remarkably Changed with the Effect of 5FU-RuNPs

Apoptosis is activated by altering the permeability of the mitochondrial membrane, which is involved in the intrinsic pathway [33]. The proteins BAX (pro-apoptotic) and BCL-2 (anti-apoptotic) determine the fate of the cell through this pathway [34]. It has also been reported that p53, a tumor suppressor gene, activates apoptosis by affecting BAX gene expression [35]. Application of 5FU-RuNPs to HCT116 cells significantly increased the protein expressions of pf Bax/Bcl-2 and p53 ($p < 0.05$). When we compare the effect

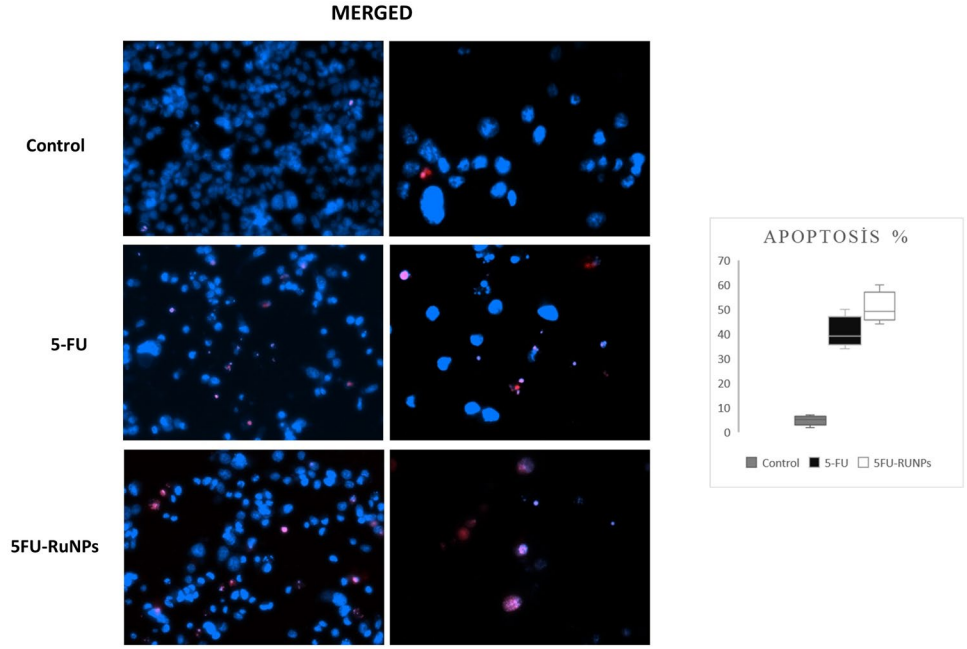

Fig. 7 Cell death was detected by immunofluorescent images in groups. According to Hoescht/ PI double staining images of HCT116 groups, apoptotic cells were seen as pink color. The magnification of the figures for each group is 20× and 40x, respectively. The percentages of apoptotic cells for each group were determined by comparison with the control group. n = 3, $p < 0.05$

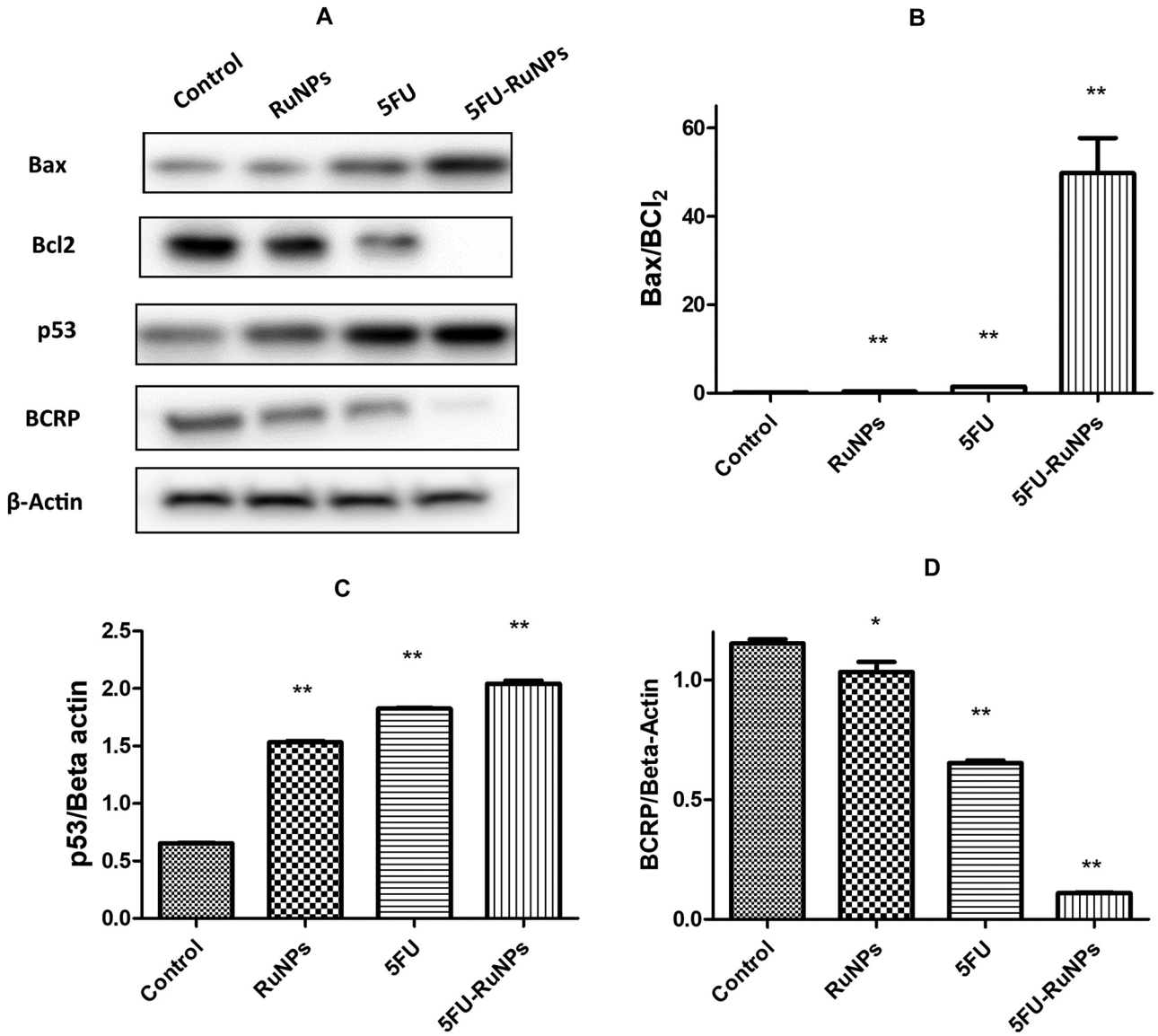

Fig. 8 In HCT116 cells the impact of RuNPs on protein expression levels of Bax/Bcl-2, p53, and BCRP are shown. Data represented as mean ± SD. *p < 0.05 compared to control cells. **p < 0.01 compared with their respective control cells

of 5FU with that of 5FU-RuNPs on colorectal cells, we see a marked increase in apoptotic proteins. (Fig. 8a–c). Therefore, in this study, we found that apoptosis occurs via the intrinsic pathway.

5FU-RuNPs Decrease the BCRP (ABCG2)-mediated Multidrug Resistance in HCT116

MDR is a very important condition that negatively affects the response to 5FU treatment in colorectal cancer, as in most cancers, and must be overcome [36, 37]. Resistance to 5FU is thought to be related to overexpression of dihydropyrimidine dehydrogenase (DPD) by breast cancer resistance protein (BCRP), also known as ABCG2, which leads to inactivation of 5FU [38]. ABCG2 also causes multidrug resistance by preventing the retention of many drugs in the cell for most treatments [39].

Membrane permeability and vascularity increase in tumor tissues. Therefore, nanoparticles between 10 and 200 nm tend to accumulate in tissues in the form of passive targeting [5]. In addition, the controlled release of the drug increases the half-life of the drug in the tumor region [40], and they also override any mechanisms that cause drug resistance by passing through the extracellular and intracellular membranes [41].

It was found that the expression of BCRP statistically decreased ($p < 0.05$). In this study, while drug resistance in the control group was quite high at baseline, interestingly,

the amount of ABCG2 decreased significantly after treatment with 5FU-RuNPs (Fig. 8d). It is suggested that Ru-based nanoparticles loaded with 5FU may be a remarkable anticancer agent for cancer therapy.

Conclusion

Clearly, the efficacy of 5FU could not be achieved due to drug resistance, and treatment of colorectal cancer failed to produce results in some patients and resulted in death. The side effects in surviving patients significantly affect their quality of life. In recent years, several studies have been conducted to minimize or eliminate the failure rate of these chemotherapeutic agents. Nanocarriers provide very successful results with their targeted and controlled release. In this study, we successfully synthesized RuNPs loaded with 5FU for the first time. Considering the release profiles of 5FU-loaded Ru nanocarriers, their cytotoxic and apoptotic effects, and their effects on drug resistance, it is believed that 5FU-RuNps may be a promising new anticancer agent in cancer therapy. We believe that the synthesized novel nanoparticles will be an enabler for further studies.

Supplementary Information The online version contains supplementary material available at https://doi.org/10.1007/s10895-023-03180-9.

Acknowledgements The manuscript has been proofread by a professional instatext editing tool (https://instatext.io/editor/?o=aa). The document was edited for proper English language, grammar, punctuation, spelling, sentence structure, phrasing, and overall style by one or more of our native (of English) academic editors.

Authors' Contributions D.Ö and F.D.K conceived and designed the analyses. All authors performed different analyzes and contributed to the data. D.Ö collected the data and wrote the paper.

Availability of Data and Materials Yes.

Declarations

Ethics Approval and Consent to Participate Yes.

Consent for Publication Yes.

Competing Interests Not Applicable.

References

1. Center MM, Jemal A, Smith RA, Ward E (2009) Worldwide variations in colorectal cancer. CA Cancer J Clin 59:366–378. https://doi.org/10.3322/CAAC.20038
2. Mir O, Brodowicz T, Italiano A et al (2016) Safety and efficacy of regorafenib in patients with advanced soft tissue sarcoma (REGOSARC): a randomised, double-blind, placebo-controlled, phase 2 trial. Lancet Oncol 17:1732–1742. https://doi.org/10.1016/S1470-2045(16)30507-1
3. Dienstmann R, Vermeulen L, Guinney J et al (2017) Consensus molecular subtypes and the evolution of precision medicine in colorectal cancer. Nat Rev Cancer 17:79–92. https://doi.org/10.1038/NRC.2016.126
4. Blunden BM, Stenzel MH (2015) Incorporating ruthenium into advanced drug delivery carriers – an innovative generation of chemotherapeutics. J Chem Technol Biotechnol 90:1177–1195. https://doi.org/10.1002/JCTB.4507
5. Subhan MA, Yalamarty SSK, Filipczak N et al (2021) Recent advances in tumor targeting via EPR effect for cancer treatment. J Pers Med 11:571. https://doi.org/10.3390/JPM11060571
6. Safwat MA, Soliman GM, Sayed D, Attia MA (2016) Gold nanoparticles enhance 5-fluorouracil anticancer efficacy against colorectal cancer cells. Int J Pharm 513:648–658. https://doi.org/10.1016/J.IJPHARM.2016.09.076
7. Javanbakht S, Hemmati A, Namazi H, Heydari A (2020) Carboxymethylcellulose-coated 5-fluorouracil@MOF-5 nano-hybrid as a bio-nanocomposite carrier for the anticancer oral delivery. Int J Biol Macromol 155:876–882. https://doi.org/10.1016/J.IJBIOMAC.2019.12.007
8. Khan S, Aamir MN, Madni A et al (2021) Lipid poly (ε-caprolactone) hybrid nanoparticles of 5-fluorouracil for sustained release and enhanced anticancer efficacy. Life Sci 284:119909. https://doi.org/10.1016/J.LFS.2021.119909
9. Jan N, Madni A, Rahim MA et al (2021) In vitro anti-leukemic assessment and sustained release behaviour of cytarabine loaded biodegradable polymer based nanoparticles. Life Sci 267:118971. https://doi.org/10.1016/J.LFS.2020.118971
10. Khan S, Madni A, Shah H et al (2022) Folate decorated lipid chitosan hybrid nanoparticles of 5-fluorouracil for enhanced anticancer efficacy against colon cancer. Int J Biol Macromol 222:497–508. https://doi.org/10.1016/J.IJBIOMAC.2022.09.196
11. Saczewski F, Dziemidowicz-Borys E, Bednarski PJ, Gdaniec M (2007) Synthesis, crystal structure, cytotoxic and superoxide dismutase activities of copper(II) complexes of N-(4,5-dihydroimidazol-2-yl)azoles. Arch Pharm (Weinheim) 340:333–338. https://doi.org/10.1002/ARDP.200700021
12. Stepanenko IN, Cebrián-Losantos B, Arion VB et al (2007) The complexes [OsCl2(azole)2(dmso)2] and [OsCl2(azole)(dmso)3]: Synthesis, structure, spectroscopic properties and catalytic hydration of chloronitriles. Eur J Inorg Chem 400–411. https://doi.org/10.1002/EJIC.200600859
13. Schott O, Ferrando-Soria J, Bentama A et al (2011) Chromium(III) complexes with 2-(2′-pyridyl)imidazole: Synthesis, crystal structure and magnetic properties. Inorganica Chim Acta 1:358–366. https://doi.org/10.1016/J.ICA.2011.06.039
14. Thangavel P, Viswanath B, Kim S (2017) Recent developments in the nanostructured materials functionalized with ruthenium complexes for targeted drug delivery to tumors. Int J Nanomed 12:2749–2758. https://doi.org/10.2147/IJN.S131304
15. Aird RE, Cummings J, Ritchie AA et al (2002) In vitro and in vivo activity and cross resistance profiles of novel ruthenium (II) organometallic arene complexes in human ovarian cancer. Br J Cancer 86:1652. https://doi.org/10.1038/SJ.BJC.6600290
16. He L, Huang Y, Zhu H et al (2014) Cancer-targeted monodisperse mesoporous silica nanoparticles as carrier of ruthenium polypyridyl complexes to enhance theranostic effects. Adv Funct Mater 24:2754–2763. https://doi.org/10.1002/ADFM.201303533
17. Xu M, Wen Y, Liu Y et al (2019) Hollow mesoporous ruthenium nanoparticles conjugated bispecific antibody for targeted anticolorectal cancer response of combination therapy. Nanoscale 11:9661–9678. https://doi.org/10.1039/C9NR01904A

18. Kasinathan K, Marimuthu K, Murugesan B et al (2021) Fabrication of eco-friendly chitosan functionalized few-layered WS 2 nanocomposite implanted with ruthenium nanoparticles for in vitro antibacterial and anticancer activity: Synthesis, characterization, and pharmaceutical applications. Int J Biol Macromol 190:520–532. https://doi.org/10.1016/J.IJBIOMAC.2021.08.153
19. Karges J, Díaz-García D, Prashar S et al (2021) Ru(II) polypyridine complex-functionalized mesoporous silica nanoparticles as photosensitizers for cancer targeted photodynamic therapy. ACS Appl Bio Mater 4:4394–4405. https://doi.org/10.1021/ACSABM.1C00151/SUPPL_FILE/MT1C00151_SI_001.PDF
20. Li Y, Shaker K, Svenda M et al (2020) Synthesis and cytotoxicity studies on Ru and Rh nanoparticles as potential X-ray fluorescence computed tomography (XFCT) contrast agents. Nanomaterials (Basel) 10. https://doi.org/10.3390/NANO10020310
21. Sethy C, Kundu CN (2021) 5-Fluorouracil (5-FU) resistance and the new strategy to enhance the sensitivity against cancer: Implication of DNA repair inhibition. Biomed Pharmacother 137:111285. https://doi.org/10.1016/J.BIOPHA.2021.111285
22. Patharkar RG, Nandanwar SU, Chakraborty M (2013) Synthesis of colloidal ruthenium nanocatalyst by chemical reduction method. J Chem. https://doi.org/10.1155/2013/831694
23. Orellana EA, Kasinski AL (2016) Sulforhodamine B (SRB) assay in cell culture to investigate cell proliferation. Bio Protoc 6. https://doi.org/10.21769/BIOPROTOC.1984
24. Kang X, Zuckerman NB, Konopelski JP, Chen S (2010) Alkyne-stabilized ruthenium nanoparticles: manipulation of intraparticle charge delocalization by nanoparticle charge States. Angew Chem Int Ed Engl 49:9496–9499. https://doi.org/10.1002/ANIE.201004967
25. Yang Y, Zhu L, Xia F et al (2017) A novel 5-FU/rGO/Bce hybrid hydrogel shell on a tumor cell: one-step synthesis and synergistic chemo/photo-thermal/photodynamic effect. RSC Adv 7:2415–2425. https://doi.org/10.1039/C6RA25834D
26. Diasio RB, Harris BE (1989) Clinical pharmacology of 5-fluorouracil. Clin Pharmacokinet 16(4):215–237. https://doi.org/10.2165/00003088-198916040-00002
27. El-Hammadi MM, Delgado ÁV, Melguizo C et al (2017) Folic acid-decorated and PEGylated PLGA nanoparticles for improving the antitumour activity of 5-fluorouracil. Int J Pharm 516:61–70. https://doi.org/10.1016/J.IJPHARM.2016.11.012
28. De MAC, Altmeyer C, Tominaga TT et al (2016) Polymeric nanoparticles for oral delivery of 5-fluorouracil: Formulation optimization, cytotoxicity assay and pre-clinical pharmacokinetics study. Eur J Pharm Sci 84:83–91. https://doi.org/10.1016/J.EJPS.2016.01.012
29. Garg A, Patel V, Sharma R et al (2017) Heparin-appended polycaprolactone core/corona nanoparticles for site specific delivery of 5-fluorouracil. Artif Cells Nanomed Biotechnol 45:1146–1155. https://doi.org/10.1080/21691401.2016.1203793
30. Chen T, Liu Y, Zheng WJ et al (2010) Ruthenium polypyridyl complexes that induce mitochondria-mediated apoptosis in cancer cells. Inorg Chem 49:6366–6368. https://doi.org/10.1021/IC100277W/SUPPL_FILE/IC100277W_SI_001.PDF
31. Li L, Wong YS, Chen T et al (2012) Ruthenium complexes containing bis-benzimidazole derivatives as a new class of apoptosis inducers. Dalton Trans 41:1138–1141. https://doi.org/10.1039/C1DT11950H
32. Dive C, Gregory CD, Phipps DJ et al (1992) Analysis and discrimination of necrosis and apoptosis (programmed cell death) by multiparameter flow cytometry. Biochim Biophys Acta 1133:275–285. https://doi.org/10.1016/0167-4889(92)90048-G
33. Dadsena S, Jenner A, García-Sáez AJ (2021) Mitochondrial outer membrane permeabilization at the single molecule level. Cell Mol Life Sci 78(8):3777–3790. https://doi.org/10.1007/S00018-021-03771-4
34. Askari N, Shafieipour S, Aghajanpour M (2019) Role of BAX, BCL-2, and MICAL-2 Genes in Esophageal Cancer
35. Yang TT, Namba H, Hara T et al (1997) p53 induced by ionizing radiation mediates DNA end-jointing activity, but not apoptosis of thryroid cells. Oncogene 14:1511–1519. https://doi.org/10.1038/sj.onc.1200979
36. Zhang N, Yin Y, Xu SJ, Chen WS (2008) 5-Fluorouracil: Mechanisms of Resistance and Reversal Strategies. Molecules 13:1551. https://doi.org/10.3390/MOLECULES13081551
37. Wu SY, Huang YJ, Tzeng YM et al (2018) Destruxin B suppresses drug-resistant colon tumorigenesis and stemness is associated with the upregulation of miR-214 and downregulation of mTOR/β-catenin pathway. Cancers (Basel) 10. https://doi.org/10.3390/CANCERS10100353
38. Alibolandi M, Hoseini F, Mohammadi M et al (2018) Curcumin-entrapped MUC-1 aptamer targeted dendrimer-gold hybrid nanostructure as a theranostic system for colon adenocarcinoma. Int J Pharm 549:67–75. https://doi.org/10.1016/J.IJPHARM.2018.07.052
39. Taylor NMI, Manolaridis I, Jackson SM et al (2017) Structure of the human multidrug transporter ABCG2. Nature 546(7659):504–509. https://doi.org/10.1038/nature22345
40. Akbarzadeh A, Rezaei-Sadabady R, Davaran S et al (2013) Liposome: Classification, preparation, and applications. Nanoscale Res Lett 8:1–9. https://doi.org/10.1186/1556-276X-8-102/TABLES/2
41. Kesharwani SS, Kaur S, Tummala H, Sangamwar AT (2018) Overcoming multiple drug resistance in cancer using polymeric micelles. Expert Opin Drug Deliv 15:1127–1142. https://doi.org/10.1080/17425247.2018.1537261

Publisher's Note Springer Nature remains neutral with regard to jurisdictional claims in published maps and institutional affiliations.

Springer Nature or its licensor (e.g. a society or other partner) holds exclusive rights to this article under a publishing agreement with the author(s) or other rightsholder(s); author self-archiving of the accepted manuscript version of this article is solely governed by the terms of such publishing agreement and applicable law.